Annals of Biomedical Engineering, Vol. 31, pp. 667–677, 2003
Printed in the USA. All rights reserved.

0090-6964/2003/31(6)/667/11/$20.00
Copyright © 2003 Biomedical Engineering Society

Expandable Bioresorbable Endovascular Stent. I. Fabrication and Properties

SHIH-HORNG SU,[1] ROBERT Y. N. CHAO,[2] CHARLES L. LANDAU,[3] KEVIN D. NELSON,[1] RICHARD B. TIMMONS,[4] ROBERT S. MEIDELL,[3] and ROBERT C. EBERHART[1,2]

[1]Joint Program in Biomedical Engineering, the University of Texas at Arlington and the University of Texas Southwestern Medical Center at Dallas, Dallas, TX ; [2]Department of Surgery and [3]Department of Internal Medicine, the University of Texas Southwestern Medical Center at Dallas, Dallas, TX; and [4]Department of Chemistry and Biochemistry, the University of Texas at Arlington, Arlington, TX

(Received 22 October 2001; accepted 10 February 2003)

Abstract—A bioresorbable, expandable poly(L-lactic acid) stent has been designed, based on a linear, continuous coil array principle, by which multiple furled lobes convert to a single lobe upon balloon expansion, without heating. Stent strength and compliance are sufficient to permit deployment by a conventional balloon angioplasty catheter. Several multiple lobe configurations were investigated, with expansion ratios ranging from 1.4 to 1.9 and expanded diameters ranging from 2.3 to 4.7 mm. Compression resistance of the expanded stent is dependent on fiber coil density and fiber ply. A range sufficient for endovascular service was obtained, with less than 4% elastic recoil in six day saline incubation studies. Surface plasma treatment with di(ethylene glycol) vinyl ether significantly reduced platelet adhesion in a 1 h porcine arteriovenous shunt model. Patency was maintained in one week implant studies in the porcine common femoral artery. However, a strong inflammatory response, and significant reduction of the vascular lumen were observed following two weeks implantation. The design principles and fabrication techniques for this bioresorbable stent are sufficiently versatile that a broad range of applications can be addressed. Much work remains to be done, including long-term evaluation of the inflammatory response, and of polymer degradation. The results of this study demonstrate the feasibility of expandable biodegradable stent design and deployment by conventional means. © *2003 Biomedical Engineering Society.* [DOI: 10.1114/1.1575756]

Keywords—Bioresorbable stent, Endovascular, Poly-l-lactic acid, Di(ethylene glycol) vinyl ether, Porcine arteriovenous shunt model, Platelet adhesion, Inflammation.

INTRODUCTION

Treatment of arterial dissection, elastic recoil, and intimal hyperplasia following percutaneous transluminal coronary angioplasty with metal stents is standard procedure, widely practiced. It is generally observed that metal stents contribute to thrombosis and inflammation[9] and induce endothelial dysfunction.[27] Rechavia *et al.* demonstrated that temporary implantation of metal stents reduced arterial narrowing,[20] suggesting that a temporary stent might reduce vessel injury and thus enhance healing. Surgical removal of an expanded metal stent *in situ* is impractical, if not impossible, since the removal procedure is extremely traumatic. As pointed out in a recent review of polymeric and metal versions,[8] stents made of bioresorbable materials would, in theory, have sufficient mechanical strength to support the vascular wall for a desired period of healing following balloon angioplasty, after which they would be gradually resorbed, as with bioresorbable suture.

Several bioresorbable stent designs have been proposed,[1,3,28] and some have been reduced to experimental practice.[5,24] Most have failed to provide suitable expansion by conventional angioplasty balloon catheter technique. Tamai *et al.*[25] first demonstrated that biodegradable poly (L-lactic acid) stents are suitable for human coronary arterial stenting. However, this unique stent required infusion of a 70 °C contrast-water mixture (approximately 50 °C at the balloon site) for expansion *in situ*, raising concerns about possible vascular necrosis.

Our group has previously demonstrated a bioresorbable stent capable of the delivery of recombinant gene transfer vectors to the arterial wall.[29] However, this device could not be deployed with a conventional angioplasty catheter; it was too stiff to maneuver in tortuous channels and would not expand suitably at the target. We have now redesigned the stent to make it more compliant, improving both maneuverability and expandability. This new design allows deployment with a conventional angioplasty balloon catheter, without heating or other unusual maneuvers. We report experimental results that demonstrate the feasibility of expandable biodegradable endovascular stents.

Address correspondence to Robert C. Eberhart, PhD, Department of Surgery, University of Texas Southwestern Medical Center at Dallas, 5323 Harry Hines Blvd., Dallas, TX 75390-9130. Electronic mail: robert.eberhart@utsouthwestern.edu

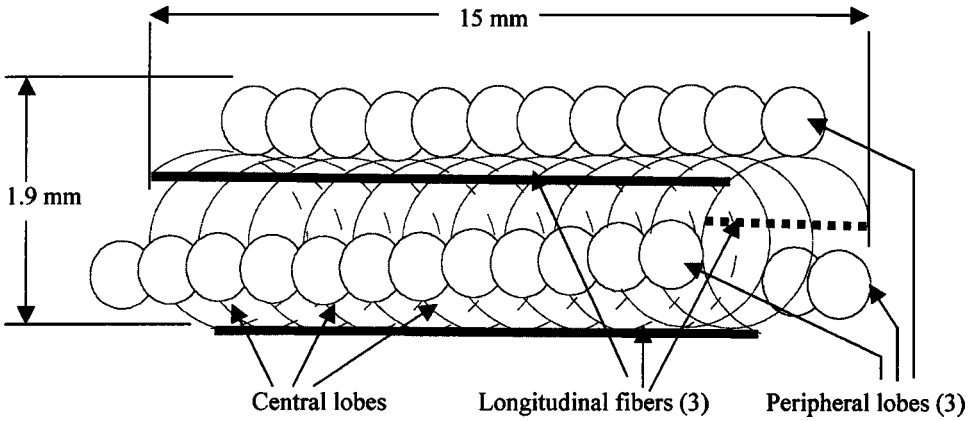

FIGURE 1. Schematic structure of an expandable biodegradable polymeric stent. The polymer stent is constructed with various numbers of coil rotations (12 in this drawing). Each rotation has one central lobe and three peripheral lobes. The central lobes form the stent backbone. Three longitudinal fibers are attached on the exterior surface of the central lobes using a viscous PLLA–chloroform solution. Typically, the length of each stent is 15 mm and the initial furled diameter is 1.9 mm; the diameter after balloon expansion is 3.2 mm and the length is unchanged. The length of the stent is readily adjusted at fabrication by increasing the number of coil rotations. The peripheral and central lobe diameters determine the final diameter of the stent. A single fiber design is depicted for clarity, however one, two or three fiber plies were used in practice.

MATERIALS AND METHODS

Preparation of Expandable Bioresorbable Stents

Poly(L-lactic acid) resin (MW_{avg} 200,000) (PLLA), was obtained from Cargill Inc., Minneapolis, MN. This branched polymer is not intended for medical applications, but was used because of its favorable strength and flexibility characteristics. The polymer was melt extruded in batch mode (Alex James, Greer, SC) and drawn 6:1 to produce 0.14-mm-diam fibers with an ultimate tensile stress of 350 ± 40 MPa. PLLA fibers 35 cm in length were woven manually around a mandrel array into a multiple coil configuration; we, typically, fabricated one central and three peripheral lobes, with three longitudinal fibers interwoven and glued to the coil for mechanical support (Fig. 1). The design also permits the peripheral lobes to be wound inside the central lobe. Once the stent was fabricated, all mandrels were removed and a conventional angioplasty balloon catheter was inserted in the main orifice. To facilitate vascular deployment the three peripheral lobes can be angled towards the central channel by a vascular sheath, which is removed upon placement at the intended site.

Influence of Mandrel Design on the Initial and Final Stent Dimensions

The initial (furled) diameter of the stent was defined as the outer (great circle) diameter of the peripheral lobes without sheathing, and before mounting on the angioplasty balloon catheter. The final diameter was defined as that obtained after balloon inflation prior to angioplasty catheter removal. Four central mandrels (rods 0.51 ± 0.01, 0.65 ± 0.01, 0.83 ± 0.01, and 1.07 ± 0.01 mm in diameter) and three peripheral mandrels (0.26 ± 0.01, 0.32 ± 0.01, and 0.39 ± 0.01 mm rods) (Small Parts, Inc., Miami Lakes, FL) were employed. Four stents were made in each combination of central and peripheral rods and were measured at three axial sites in triplicate, before and after balloon expansion (Table 1). The balloon inflation system consisted of the Diamond™ Balloon Dilation Catheter (1.8–4.0 mm OD) and the Encore 26 Inflator (Boston Scientific/Medi-tech, Boston, MA). Inflation pressures ranged from 3 to 10 atm.

Mechanical Properties: Inflation Pressure, Recoil, and Radial Compression Resistance

Five stents with initial external diameters of 1.9 ± 0.02 mm were prepared and stored in a desiccator for one week prior to use. The OD of the furled, unsheathed stent was measured with a Vernier caliper, and then remeasured in triplicate as a function of increasing inflation pressure at 1 atm increments from 1 to 10 atm.

For the stent recoil studies, four fully expanded stents (average final diameter, 3.6 ± 0.04 mm, measured before the removal of the deflated balloon) were detached from the balloon catheter and incubated in 50 mM PBS (pH 7.2) at 37 °C. The stent was removed from the saline solution, the OD was measured and the stent was replaced in the solution, at 20 min, and 24, 48, 120, and 144 h following the initial incubation.

The influences on mechanical compressive strength of the number of coil turns (coil density) and the number of fibers in each coil turn (fiber ply) were studied in separate radial compression tests. A radial compression chamber, measuring the radial inward buckling (collapse) pressure was adapted for this purpose.[29] The collapse

TABLE 1. Initial and final diameters of expandable stent designs.

Rod		Peripheral								
		0.26±0.01			0.32±0.01			0.39±0.01		
	Rod size (mm)	Initial diameter of stent	Final diameter of stent	Expansion ratio	Initial diameter of stent	Final diameter of stent	Expansion ratio	Initial diameter of stent	Final diameter of stent	Expansion ratio
	0.51 ± 0.01	1.60 ± 0.27	2.35 ± 0.34	1.46	2.0 ± 0.18	2.9 ± 0.40	1.45	1.85 ± 0.36	3.05 ± 0.61	1.65
Central	0.65 ± 0.01	1.63 ± 0.15	2.60 ± 0.30	1.59	2.10 ± 0.08	3.15 ± 0.06	1.50	2.01 ± 0.12	3.49 ± 0.21	1.73
	0.83 ± 0.01	1.70 ± 0.03	2.82 ± 0.02	1.65	2.04 ± 0.05	3.34 ± 0.04	1.64	2.26 ± 0.01	3.83 ± 0.01	1.69
	1.07 ± 0.01	2.15 ± 0.03	3.25 ± 0.03	1.51	2.30 ± 0.01	3.57 ± 0.01	1.55	2.42 ± 0.01	4.70 ± 0.03	1.94

Note: Initial and final diameter of the expandable stent vary with different combinations of the central and peripheral mandrel rod diameters. Numbers are expressed in mm as mean±SD.

pressure was analyzed for stents with various coil densities (12, 15, and 18 turns in 15 mm length segments) and fiber plies (1, 2, and 3 ply with 12 turn coils). All stents were balloon expanded at a pressure of 10 atm before the collapse pressure test commenced.

Surface Treatment for Thromboresistance

Following fabrication, stents were treated with di(ethylene glycol) vinyl ether, $H_2C{=}CH(OCH_2CH_2)_2OH$ (hereinafter referred to as EO2V, Aldrich, Milwaukee, WI) using a pulsed plasma polymerization technique.[30] Briefly, stents were cleaned by ultrasonication in 70% alcohol for 20 min, three times, followed by vacuum drying for 4 days at 45 °C. One day before the plasma treatment, the reactor chamber was cleaned with acetone, followed by oxygen plasma treatment overnight to remove any residue from previous experiments. Before plasma polymerization, the system was evacuated to a background pressure of approximately 5 mTorr. Next, argon was bled into the chamber at a pressure of 0.8 Torr. A 5–10 min pulsed Ar plasma (100 W rf absorbed power and a duty cycle of 10 ms on/100 ms off), was used to clean the stent surface. After this cleaning step, the Ar flow was terminated and the system was again evacuated to background pressure. EO2V was then introduced into the reaction chamber. After the establishment of a monomer flow rate of 0.9 cm^3/min and a pressure of 30–40 Torr, the polymerization reaction was initiated at a total absorbed rf power of 100 W.

The stent thromboresistive characteristic was tested in an *ex vivo* femoral arterio-venous porcine shunt model, employing radiolabelled platelets. The use and care of animals conformed to DHHS Guidelines as published in (NIH) 85-23 DRR/NIH, Bethesda, MD. Stents were implanted in separate 200 mm long, 0.30 mm ID silicone rubber tubes (one for controls, one for EO2V-treated stents). Six 15 mm long stents were placed in each tube at 15 mm intervals, no less than 70 mm distant from the tube ends. The tubes had sufficient compliance to permit insertion and retention of the stents at their intended positions. The stented silicone rubber tubes were immersed in 70% alcohol solution for 4 h for sterilization and rinsed with 0.9% saline before experiment. Freshly drawn blood from 40 to 50 kg ($n=4$) domestic pigs was processed for platelet isolation and radiolabeling with ^{111}In-oxime, employing the modified procedure of Thakur and Welch.[26] While the platelets were being labeled the animals were intubated and maintained on a ventilator with oxygen enrichment and isoflurane anesthesia. The inguinal region was prepared, the femoral artery and vein were exposed and mobilized bilaterally and two femorofemoral arteriovenous shunts were created. Once the specific radioactivity of the ^{111}In platelets was measured, the platelet concentrate was injected and allowed to circulate for 30 min. At this point the silicone A–V shunts were introduced bilaterally. Blood flow through the shunts was monitored by an ultrasonic flow probe (Transonic, Ithaca, NY) and maintained for 1 h at 200–250 ml/min. Shunts were then removed, gently

rinsed with saline, then stents were dissected and preserved in 10% PBS-buffered formaldehyde. The procedure was then repeated with other stents assembled in fresh silicone rubber sections. No more than four test sections were investigated in a single experiment. The circulating platelet count was monitored throughout the test period, in order to correct for platelet dilution. Stent radioactivity was then measured using a gamma counter (Universal Gamma Counter, 1282 Compugamma, LKB). After counting, stents with adherent cells were prepared for scanning electron microscopy (SEM, JEOL model JSM 840A, Peabody, MA).

In Vivo Stent Implantation in the Common Femoral Artery

Stents, four each, with or without EO2V coating, were prepared and sterilized with ethylene oxide gas, one day before implantation. Adult domestic pigs ($n=4$) were administered oral aspirin (325 mg) and ticlopidine (250 mg) daily for 4 days before surgery. On the test day, following sedation with ketamine (20 mg/kg IM) and atropine (0.07 mg/kg IM), animals were ventilated by mask with an air/O_2 mixture and administered isoflurane 0.5%–21% for maintenance anesthesia. Animals then received 5,000 U heparin IV. Following surgical exposure, a 10F introducer sheath was positioned in the left common carotid artery. All catheters (including guidewire, guiding catheter and dilation catheter) were subsequently introduced through this sheath and advanced to the common femoral artery. An EO2V coated stent was mounted on an angioplasty balloon catheter and positioned in the common femoral artery by passage over a 0.014 in. guidewire. The balloon was then inflated to 10 atm for 1 min, and removed 30 s after deflation. The implantation of the stent was then repeated in random order on the contralateral vessel with an uncoated (control) stent. Following removal of ancillary equipment and sterile closure, animals were permitted to recover, were observed daily and treated as necessary. All animals received daily cefazolin (500 mg, IV or IM) for three days. On the 7th or 14th postoperative day, animals were sacrificed with a lethal dose of intravenous sodium pentobarbital (150 mg/kg). A cannula was immediately inserted into the infrarenal abdominal aorta, and vessels were perfusion fixed with 10% buffered formalin at 120 mm Hg pressure. Stents, including generous margins of adjacent vessel were harvested and stored in 10% buffered formalin. Stents were then segmented, embedded in paraffin, sectioned by microtome and stained with hematoxylin and eosin.

RESULTS

Figures 1 and 2 demonstrate how the three peripheral lobes provide the extra length of fiber needed for complete balloon expansion to a single central lobe. The fully expanded stent structure is a helical coil with three longitudinal reinforcing fibers. Using one central and three peripheral rod mandrels, the furled diameters of stents first produced in this fashion ranged from 1.6 ± 0.05 to 2.42 ± 0.01 mm. The expanded stent diameters ranged correspondingly from 2.35 ± 0.04 to 4.7 ± 0.03 mm, with expansion ratios ranging from 1.45 to 1.94 (Table 1). Stent length did not change upon expansion, owing to the support of the axial reinforcing fibers.

We selected 0.65 and 0.32 mm, respectively, for the central and peripheral rod mandrel diameters to fabricate the stents reported in this work. We sought to provide a high expansion ratio, enabling deployment of low profile, furled stents through narrow and tortuous channels, yet providing an adequately large expanded diameter to approximate the lumen of the instrumented vessel. In practice, the stent expanded diameter was the more important design criterion since the target vessel for this study, the midregion of the porcine common femoral artery, is not that difficult to negotiate and is, nominally, 3 mm in diameter. Since the actual vessel diameter may differ, and since a slight compression is desired to maintain position stability once deployed, the expanded diameter of the stent was specified to be 10% larger, 3.3 mm. Stents used for most tests were made with the combination of 0.65 and 0.32 mm rod mandrels, yielding an expanded diameter of 3.24 mm, close to the desired expansion. Stent length was adjusted as needed by simply changing the number of coil rotations and reinforcing longitudinal fiber length.

The expanded diameter of the stent increased promptly with applied inflation pressure, reaching a maximum of 3.24 mm at 3 atm and maintaining that diameter without further deformation at pressures up to 10 atm. The experiment was stopped at 10 atm because of the limitation of our inflation device.

A small amount of stent radial recoil was observed. Larger diameter stents (3.62 ± 0.04 mm) were prepared for this test in order to more accurately measure the extent of recoil. Stent diameter decreased 2%, not statistically significant, in the first 20 min after the removal of the balloon catheter. After 48 h, the diameter had decreased an additional 2% ($p=0.04$). No further shrinkage was detected through 144 h of incubation: The average final stent diameter was 3.50 ± 0.05 mm.

The radial collapse pressure was linearly proportional to the coil density. As the coil density increased from 0.8 to 1.2 turns/mm, the required collapse pressure increased approximately 125%, from 16.2 ± 2.9 to 19.9 ± 1.0 psi. The fiber ply significantly influenced the mechanical per-

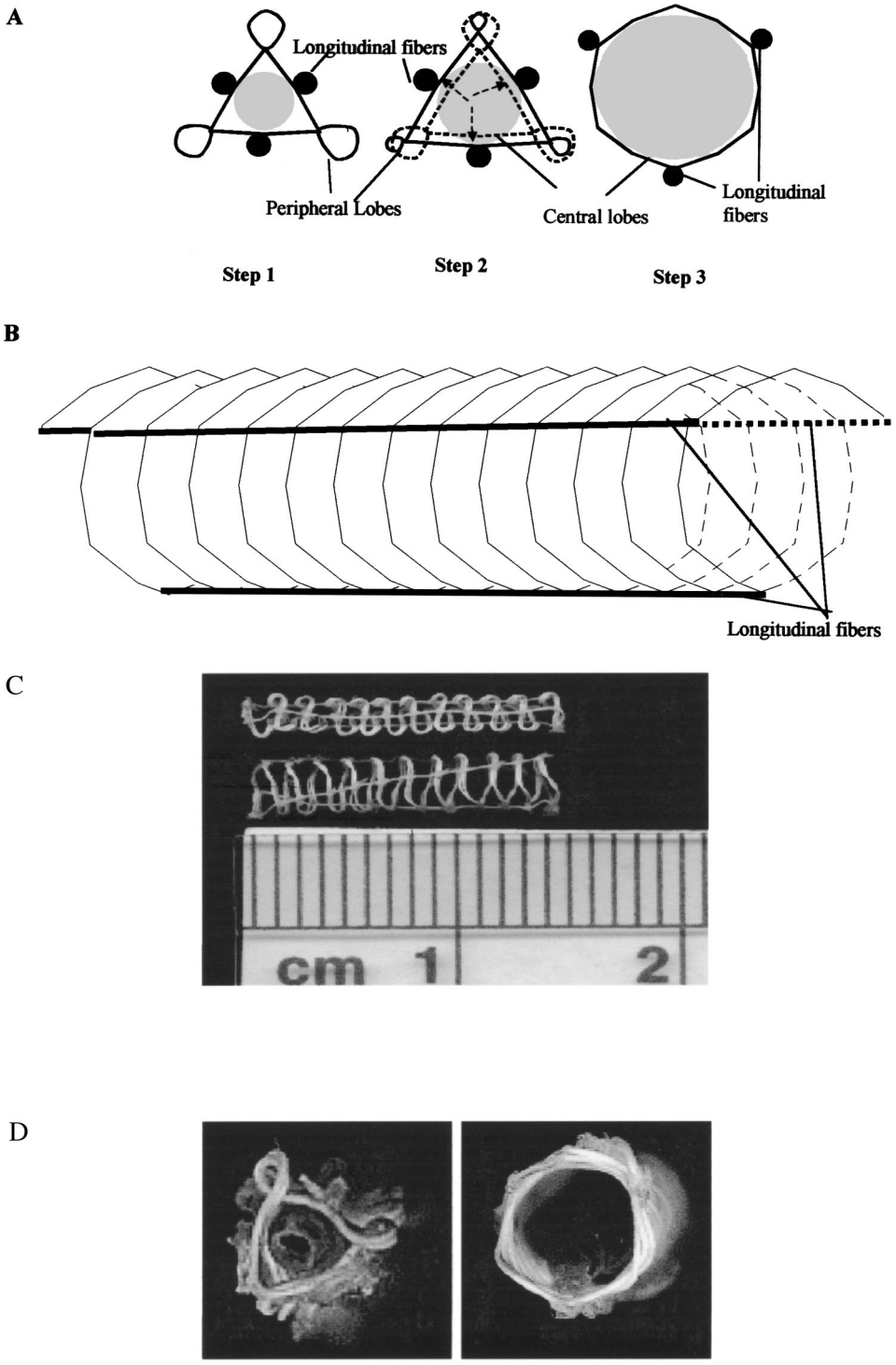

FIGURE 2. Cross-sectional diagram of stent expansion (A), transverse diagram of expanded stent (B), and photographs of the results [(C) and (D)]. (A) Step 1. The stent is mounted on an angioplasty catheter balloon; the shaded region represents the deflated balloon. Step 2. Balloon pressurization causes fiber to be transferred from the peripheral lobes to the central lobe. Arrows indicates stent expansion in the radial direction. Step 3. Only an enlarged central lobe exists after the balloon is fully inflated. (C) Side view of furled (upper) and expanded (lower) two-ply fiber stent. (D) End-on furled, 1.9 mm OD (left) and expanded 3.2 mm OD (right) views of the same stent.

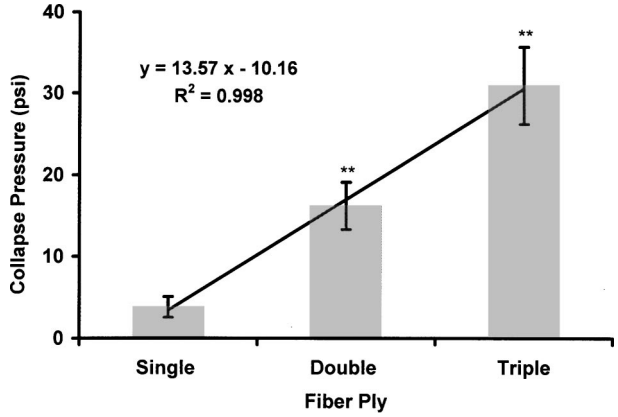

FIGURE 3. Influence of fiber ply on collapse pressure; $n = 4$, mean ± SD; $^{**}p < 0.01$.

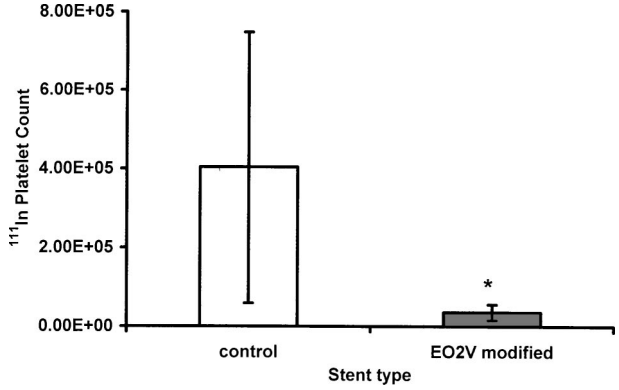

FIGURE 5. Adherent ^{111}In-labeled platelet count on the stent surface. Twelve stents (6 control, 6 EO2V coated) were tested in each of four pigs. Isotope activity was averaged for all six stents in each group, for each pig, thus $n = 24$. The displayed value is the mean ± SD of the four individual averages; $^{*}p < 0.01$.

formance of the expanded stent (Fig. 3). The radial collapse pressure increased 714% (3.8 ± 1.3–30.9 ± 1.7 psi) as the fiber ply increased from 1–3.

Figure 4 presents the ^{111}In-labeled platelet distributions in the A–V shunt experiments. There were progressive increases in platelet adhesion in both groups with stent position, with the largest number of adherent platelets observed at the sixth position. Adherent platelet numbers were lower for the EO2V treatment group than for controls at all save the two proximal positions, although differences were not statistically significant at any position. However, when averaged over all six positions, a significant reduction in ^{111}In-labeled platelet adhesion with EO2V treatment was obtained (91%, $p < 0.05$) (Fig. 5). These findings were supported by SEM observation of stent pairs placed at the shunt midpoint (position 3), both harvested from same animal [Figs. 6(A) and 6(B)]. Both isolated and aggregated platelets were, typically, visible on the surface of the control stent; phagocytic cells with extending pseudopodia were also observed [Fig. 6(A)]. Fewer single platelets and aggregates were typically observed on EO2V-treated stent surfaces [Fig. 6(B)]. Some activated phagocytic cells were also seen. Taken together, the radiolabel and SEM results demonstrate that the EO2V coating reduces platelet adhesion for the 1 h study period.

The deployability (deliverability and expandability) of the stents, observed during placement, was confirmed by *in vivo* angiography of the common femoral arteries. No

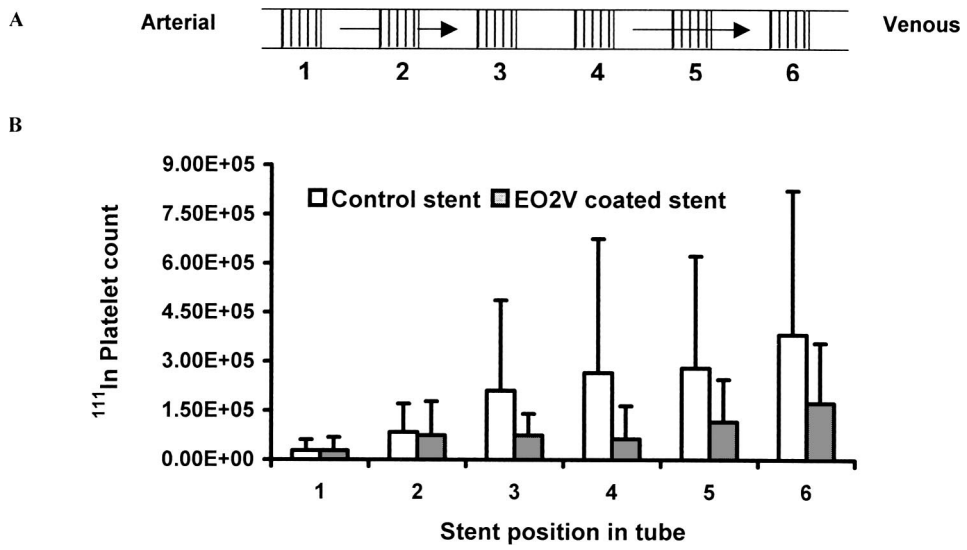

FIGURE 4. Dependence of platelet adhesion on stent position within the silicone rubber tube; $n = 4$, mean ± SD. A. Stent position diagram; six 15 mm stents were placed at 15 mm intervals, no less than 70 mm distant from the tube ends; arrows indicate the blood flow direction. (B) Mean adhesion of indium-labeled platelets at different positions Error bars indicate SEM.

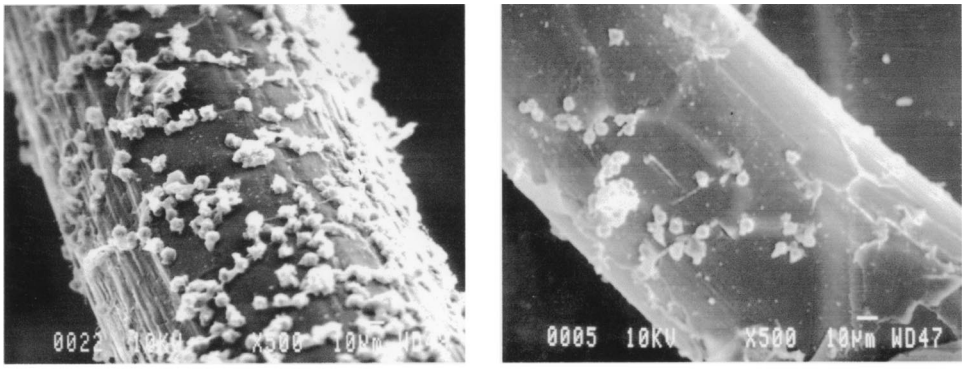

FIGURE 6. SEM of adherent blood cells on control (A) and EO2V-treated (B) PLLA stent surfaces. Both stents, harvested from same animal, were located at silicone tube position 3. Pictures were taken of the longitudinal fibers from the interior surface, oriented toward the tube lumen. Platelet clusters and some activated phagocytic cells (with extended pseudopodia) are visible in (A). In (B), fewer platelet clusters and activated phagocytic cells appear.

downstream migration of the deployed stents was observed at one week; one stent migrated in the two-week implantation group.

Examination of the samples harvested at one week following placement revealed, for both control- and EO2V-treated stents, patent channels and lumenal surfaces that appeared to be well endothelialized. A mild inflammatory response was observed, with a thickened medial layer, containing few PMNs or giant multinucleated cells [Figs. 7(A) and 7(B)]. Results were different at two weeks. One control stent was patent and well covered with endothelium. However, a severe inflammatory response was observed for this and the contralateral, EO2V-treated stent, which was not endothelialized [Figs. 7(C) and 7(D)]. Stent struts in both cases were surrounded by PMNs, plasma cells, giant multinucleated cells, and extracellular matrix. A thickened medial layer was observed, with 90% reduction of the cross section.

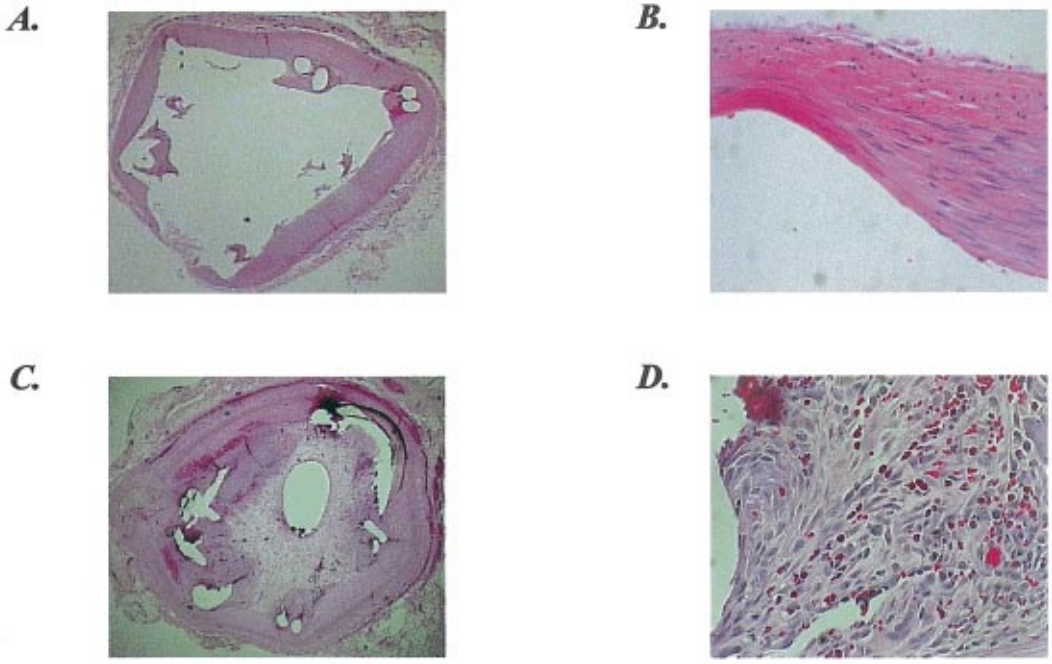

FIGURE 7. Stent implantation histology. (A) Left common femoral artery with EO2V treated stent, one week implantation, 20×magnification. (B) 400×magnification of specimen in (A) indicates PMN and giant multinuclear cells in a thickened SMC layer. (C) Right common femoral artery with an untreated control stent, two week implantation, 20×magnification. Similar findings were observed for EO2V treated stents at two weeks. (D) 400×magnification of specimen in (C) indicates inflammatory cells in the neointimal layer. All specimens were stained with hematoxylin and eosin.

In addition to the severe inflammatory response, focal intramural hemorrhage was evident on the one nonpatent stent; this stent had migrated 7 mm downstream.

DISCUSSION

Stent Design

Biodegradable and nondegradable versions of all-polymer stents have long been advocated.[14] Most of the initial designs had a tubular shape with a solid wall in order to provide sufficient strength against the radial compressive forces of the vessel, or to serve as a reservoir for drug delivery. Progress in tubular stent development was hindered by limited expandability. More recent, fiber-based designs have employed a combination of induced- and shape memory-based expansion, the latter requiring heating to set the polymer. We employed a different fiber design principle, constructing a furled stent with central and peripheral lobes, which provides several advantages.

Peripheral Lobes Provide Extra Fiber for the Expansion of the Central Lobe. A major difference between metal and polymeric stent materials is that the metals are more malleable and can be deformed without adversely affecting mechanical strength. Polymer wires cannot retain mechanical strength following permanent bending without extraordinary measures, as in the case of *in situ* thermal treatment.[25] Our approach overcomes the inability of the polymer to support a permanent bend, taking advantage instead of the flexibility provided by a multiple loop polymeric coil. The extra length of fiber, and its flexibility during expansion removes the need for permanent deformation. Once the desired final length of polymer fiber is known, the stent can be prepared with that length in a furled, multiple lobe configuration. After expansion, the desired open mesh cylindrical structure of specified diameter is obtained and maintained at clinically relevant ballooon expansion pressures. There is a small amount of torsional preload in the current design which, upon expansion, angles the longitudinal reinforcing fibers to the stent axis. However, there is minimal change in axial length, no permanent fiber deformation and no loss of cylindrical structure, all of which are important for proper stent placement.

An immediate question in this approach is, how to minimize the stent initial diameter, since extra fiber must be provided. The partial answer is to divide one large lobe into a small central lobe and three peripheral lobes. However, it may be necessary to also slant the peripheral lobes inwards, towards the central axis, to reduce the furled diameter. In this original series it was not necessary to slant the peripheral lobes or sheath the assembly, because the torsional preload on the fibers inclined the peripheral lobes sufficiently to allow the stent to pass through the guiding catheter. If this design is proved to be clinically feasible, removal of the torsional preload will be necessary, requiring inward bending of the peripheral lobes, and a retractable sheath, to avoid traumatic contact of the peripheral lobes with the vessel wall. Another approach that we have recently verified, involves winding the peripheral lobes within the central lobe. The profile is considerably smaller during deployment, but greater deformation of the fibers during expansion is required to obtain a smooth circular cross section.

Longitudinal Fibers Provide Support for the Flexible Coil. Solid wall tubular stents are not optimized for passage through small caliber, tortuous vessel networks, nor can they accommodate branch vessels, both features limiting their use. This fiber-based design can permit blood flow to branch vessels, and can maintain integrity during delivery by virtue of the longitudinal supporting fibers. This provides the inherent flexibility of a coil design without hindering expansion, thus making the stent competitive with metal models and also broadening the applications to other body conduits. While three longitudinal reinforcing fibers are provided in this case, arranged at 120° intervals, the number can be varied to suit, based not only on strength criteria but also on other factors, such as drug reservoir capacity.

Stent Delivery and Deployment System is Based on Conventional Angioplasty Balloon Catheters. By employing the same or similar deployment techniques as current clinical practice, the learning curve is shortened, established clinical principles and experience are invoked, and clinical acceptance is fostered.

Mechanical Performance

Mechanical performance is a major challenge for polymeric stents, which is met by this design. The stent was promptly and fully expanded at relatively low pressure (3 atm), and maintained the same expanded configuration over a broad range of inflation pressures (3–10 atm). We believe higher pressurization is feasible; this may be important since some (older) recommendations for expansion specify higher inflation pressures, sometimes 16–20 atm. However, it is unclear whether or not high balloon inflation pressures improve the long-term clinical outcome.[6] Recent metal stents are designed to limit deployment pressure to 5 atm or less.

A high compression collapse pressure is desired in order to reliably support the blood vessel. Stent coil density (number of turns) and fiber ply significantly influenced this property of the bioresorbable stent, permitting achievement of collapse pressures in the same range as observed with recent metal stent designs. However, collapse pressure is not the only criterion for practical

stent usage. High coil density, and high fiber ply both increase stent stiffness, making it more difficult to maneuver through the blood vessels. Furthermore, these stiffer stents require an increased inflation pressure for full deployment. Designing for low-pressure deployment would follow the clinical trend, and is recommended.

There is no ready answer for the question of ''how much compression resistance is enough?'' Rieu *et al.*[23] tested the mechanical performance of 17 current intracoronary stent designs *in vitro*. No expanded stent deformed noticeably at radial compression pressures up to 3×10^4 Pa (0.3 atm). Beyond that pressure, stent compression performance differed. This study hints at the answer to the question. Since the 17 metal stents were already clinically ''proven'' to be capable of maintaining coronary artery patency, 3×10^4 Pa may be considered to be the minimum required compression resistance. The current polymeric stent design passes this minimum requirement. Thus, there may be no need to pursue higher collapse pressure by sacrificing expandability and flexibility.

The retention of strength during degradation is a central question for bioresorbable stents. We produced PLLA fibers from the same resin batch and 0.6 mm spinneret, extruded at 240 °C and drawn 4:1–6:1. These fibers were incubated in 37 °C saline for periods up to 9 weeks (Anagha Phansalkar, MS thesis, University of Texas at Arlington, 1997). We found no loss in fiber tensile strength or helical coil radial compressive strength, and 4.4% mass loss, following incubation. These results appear to track published experience.[10]

EO2V Coating Inhibits Platelet Adhesion

Several factors influence platelet adhesion to the stent fibers in the *ex vivo* shunt experiment: (1) the hemostatic status of the animal; (2) contact activation of the platelet adhesion system by the foreign material (both stent and silicone tubing); and (3) flow-induced thrombus formation.[17] We sought to minimize the first factor by careful animal preparation and incorporation of several stents in replaceable shunt tubes, thereby reducing the number of experiments. Despite these measures the major cause of variance in this study is intra-subject variation. The mean values for adherent ^{111}In-labeled platelets are $4.04\times10^5\pm3.45\times10^5$ and $3.55\times10^4\pm2.01\times10^4$ (mean$\pm$SD) for the control and EO2V coated stent groups, respectively; the corresponding coefficients of variation are 0.854 and 0.567. If the results for individual series are divided by the baseline (preexposure) circulating platelet count, the normalized cumulative platelet adhesion rates for the control and EO2V stents become 0.126 ± 0.027 and 0.027 ± 0.003, respectively; the corresponding coefficients of variation, 0.213 and 0.096, are much improved.

Both stent fibers and silicone tubing contribute to thrombus formation in this setting. We have observed significant platelet adhesion to silicone rubber tubing in porcine *ex vivo* gamma imaging studies of membrane oxygenators.[15] There is a 70 mm silicone tubing run-in prior to platelet contact with the first stent, thus it is likely that platelets were activated before the first stent was encountered. Such activated platelets are prone to reattachment.[7,13]

Flow disordering is a sensitive feature of this experiment. The expanded stent fibers contact the shunt tubing orthogonal to the tube axis, disturbing the axial flow and creating eddies proximal and distal to the fiber. The entrapment of platelets in such ''flow step'' regions has been described.[12] Platelet activation is enhanced by disturbed axial flow[2] and by sequestration in trapped eddies, where platelet release reaction and clotting factor products can accumulate.[21,22] Sheng (MS Thesis, UT Southwestern, 2002), employed a silicone tubing flow loop and whole blood to examine the circumferential distribution of adherent platelets around PLLA fibers. He noted a high concentration of platelet aggregates and thrombi at the contact point of the fiber with the tube, and a low concentration at the free surface of the fiber. This line of thrombus was observed over the length of the PLLA fiber. His observations support the notion that platelet aggregates form and attach in trapped eddies in the fiber-tube wall contact region. They are also consistent with the idea that ejected platelet emboli can reenter and attach at downstream trapped eddy sites. Taken together, these concepts can explain the progressive increase in platelet adhesion with stent position down stream (Fig. 4). Furthermore, the differences in platelet adhesion between EO2V treated and control stents at a specific position, while nonsignificant, nevertheless reflect the ability of the coating to inhibit platelet attachment, by von Willebrand factor and/or fibrinogen ligands,[11] under reactive conditions. When analyzed by repeat measures over all tube positions (Fig. 5), the treatment-induced difference becomes statistically significant. The similarity of results between EO2V-coated and control stents at positions 1 and 2 might be explained by relatively low concentrations, and reactivity, of flow-disturbed platelets.

Examination of the typical SEM images of the free surface of the fiber at position 3 (Fig. 6) showed a clear distinction between EO2V-treated and control fibers. This examination focused on the region of the fiber least likely to be influenced by recirculation. One might argue that high fluid shear at the free surface of the fiber might detach adherent platelets. However, the same effect would be seen in both groups, since blood flow rates were matched. It is significant that the shapes of those platelets attached to the treated surface were more rounded in appearance than those on controls, suggesting lower activation and less adhesiveness.[19] Therefore, the

shear-induced effect could not have been dominant, further supporting the hypothesis of a beneficial effect of the surface treatment. Thus, the radiolabeled platelet measurements and the SEM observations both support the effectiveness of EO2V treatment in inhibiting platelet attachment to the stent fibers, both in regions of disturbed flow (fiber–tube contact) and flow ordering (free surface).

The one-week stent implantation study provides only limited discrimination of thrombus formation between treated and untreated surfaces. Large numbers of platelet thrombi were not observed on the sectioned surfaces, and the EO2V-treated stents were indistinguishable from untreated controls. The fragmented material adjacent to stent fibers in the Fig. 7 micrographs is an artifact of sample sectioning, not evidence of platelet thrombi. There might have been inhibition of the thrombogenic response on both treated and control surfaces by one week as a result of selective protein adsorption.[18] By that time the protein-rejecting EO2V coating might have eroded or been overcome by competitive protein adsorbates. The two week implantation results are not relevant to the thrombogenicity discussion, owing to the overriding inflammatory response. Thrombogenicity certainly influences patency, and surface-induced thrombogenicity of implants is observed for years.[4] However, thrombogenicity is generally not the primary consideration after the first 24–48 h following device implantation.[4]

The branched PLLA structure was obtained with an epoxide functionality. We assume that all reactant was consumed during polymerization. However, residual epoxide may have influenced the host response in the *ex vivo* and *in vivo* experiments. Purification of PLLA has produced significantly improved results in recent experiments.

Inflammation is the Dominant Host Response

Acute and subacute stent restenosis has become less common nowadays, due in part to improvements in stent design and deployment techniques, aggressive antiplatelet therapy, and the advent of anti-inflammatory drug-eluting metal stents, which have recently shown considerable promise for the inhibition of neointimal proliferation and stenosis.[16] Our results from the one and two week *in vivo* studies gave no signs of overt thrombosis. As observed in the histology study, the reduction of patency suggests strong inflammatory activity, unmasked from the thrombotic tendencies of the bioresorbable material. The *in vivo* series was terminated at two animals because of the impressive proliferative response. Clearly, the aspect of the host response most resistant to treatment in our initial experimental series is inflammation.

CONCLUSION

A bioresorbable stent based on a continuous multiple fiber coil array has been designed, with sufficient strength and compliance to permit maneuvering and expansion with a conventional balloon angioplasty catheter. A series of triple-peripheral lobe configurations were investigated. Stent expansion ratios from 1.4 to 1.9 were obtained, with expanded diameters ranging from 2.3 to 4.7 mm. The compression resistance of the expanded stent is dependent on fiber coil density and fiber ply, and covers a range sufficient for endovascular service. There is less than 4% elastic recoil of unloaded stents in six day saline incubation studies. Surface treatment with EO2V significantly reduced platelet adhesion in a porcine one-hour arteriovenous shunt model. Prototype stents were deployed in the porcine femoral artery for one and two week periods. All but one stent remained at the deployment site. Patency was maintained at one week, but lumen dimensions were significantly reduced at two weeks, due to a strong inflammatory response. The design and fabrication principles are sufficiently versatile that a broad range of applications can be addressed. The results of this study demonstrate the feasibility of expandable biodegradable endovascular stent design and deployment by conventional means, without heating. Much work remains to be done, including long term evaluation of the inflammatory response, and of polymer degradation. But the door is open for studies of temporary stent implantation.

ACKNOWLEDGMENT

The authors gratefully acknowledge support from NIH Grant No. R01 HL/DE 53225.

REFERENCES

[1] Agrawal, C. M., and H. G. Clark. Deformation characteristics of a bioabsorbable intravascular stent. *Invest. Radiol.* 27:1020–1024, 1992.

[2] Barstad, R. M., U. Orvim, M. J. Hamers, G. E. Tjonnfjord, F. R. Brosstad, and K. S. Sakariassen. Reduced effect of aspirin on thrombus formation at high shear and disturbed laminar blood flow. *Thromb. Haemostasis* 75:827–832, 1996.

[3] Blindt, R., K. M. Hoffmeister, H. Bienert, H. Pfannschmitt, G. Bartsch, H. Thissen, D. Klee, and J. Von Dahl. Development of a new biodegradable intravascular polymer stent with simultaneous incorporation of bioactive substances. *Int. J. Artif. Organs* 22:843–853, 1999.

[4] Clagett, G. P., and R. C. Eberhart. Artificial devices in clinical practice. Hemostasis and Thrombosis: Basic Principles and Clinical Practice, 3rd ed., edited by R. W. Colman, J. Hirsh, V. J. Marder, and E. W. Salzman. Philadelphia, PA: Lippincott, 1994, Chap. 77, pp. 1486–1505.

[5] De Scheerder, I. K., K. L. Wilczek, E. V. Verbeken, J. Vandorpe, P. N. Lan, E. Schacht, J. Piessens, and H. De Geest.

Biocompatibility of biodegradable and nonbiodegradable polymer-coated stents implanted in porcine peripheral arteries. *Cardiovasc. Intervent. Radiol.* 18:227–232, 1995.

[6] Dirschinger, J., A. Kastrati, and F. J. Neumann. Influence of balloon pressure during stent placement in native coronary arteries on early and late angiographic and clinical outcome: A randomized evaluation of high-pressure inflation. *Circulation* 100:918–923, 1999.

[7] Dollar, M. L., M. K. Sly, R. G. Credi, A. Constantinescu, C. C. Tsai CC, P. V. Kulkarni, G. P. Clagett, and R. C. Eberhart. Noninvasive quantification of platelet accumulation and release on indwelling venous catheters. *ASAIO J.* 39:M268–M272, 1993.

[8] Eberhart, R. C., S-H. Su, K. T. Nguyen, M. Zilberman, L. Tang, K. D. Nelson, and P. Frenkel. Bioresorbable polymeric stents: Current status and future prospects. *J. Biometer. Sci: Polymer Ed.* (in press).

[9] Farb, A., G. Sangiorgi, A. J. Carter, V. M. Walley, W. D. Edwards, R. S. Schwartz, and R. Virmani. Pathology of acute and chronic coronary stenting in humans. *Circulation* 99:44–52, 1999.

[10] Grizzi, I., H. Garreau, S. Li, and M. Vert. Hydrolytic degradation of devices based on poly(DL-lactic acid size dependence). *Biomaterials* 16:305–311, 1995.

[11] Houdijk, W. P., K. S. Sakariassen, P. F. Nievelstein, and J. J. Sixma. Role of factor VIII-von Willebrand factor and fibronectin in the interaction of platelets in flowing blood with monomeric and fibrillar human collagen types I and III. *J. Clin. Invest.* 75:531–540, 1985.

[12] Karino, T., H. L. Goldsmith, M. Motomiya, S. Mabuchi, and Y. Sohara. Flow patterns in vessels of simple and complex geometries. *Ann. N.Y. Acad. Sci.* 516:422–441, 1987.

[13] Kinlough-Rathbone, R. L., and D. W. Perry. Prolonged expression of procoagulant activity of human platelets degranulated by thrombin. *Thromb. Haemostasis* 74:958–961, 1995.

[14] Labinaz, M., J. P. Zidar, R. S. Stack, and H. R. Phillips. Biodegradable stents: The future of interventional cardiology? *J. Intervent. Cardiol.* 8:395–405, 1995.

[15] Li, J., M. K. Sly, R. Chao, A. Constantinescu, P. V. Kulkarni, F. H. Wians, Jr., M. E. Jessen, and R. C. Eberhart. Transient adhesion of platelets in pump-oxygenator circuits: Influence of SMA and nitric oxide treatments. *J. Biomater. Sci., Polym. Ed.* 10:235–246, 1999.

[16] Morice, M., P. W. Serruys, J. E. Sousa, J. Fajadet, E. Ban Hayashi, M. Perin, A. Colombo, G. Schuler, P. Barragan, G. Guagliumi, F. Molnar, and R. Falotico (RAVEL Study Group). A randomized comparison of a sirolimus-eluting stent with a standard stent for coronary revascularization. *N. Engl. J. Med.* 346:1773–1780, 2002.

[17] Morton, W. A., and R. D. Cumming. A technique for the elucidation of Virchow's triad. In: The Behavior of Blood and its Components at Interfaces. L. Vroman and E. F. Leonard, Eds. *Ann. N.Y. Acad. Sci.* 283:477–493, 1977.

[18] Nojiri, C., T. Okano, H. Koyanagi, S. Nakahama, K. D. Park, and S. W. Kim. *In vivo* protein adsorption on polymers: Visualization of adsorbed proteins on vascular implants in dogs. *J. Biomater. Sci., Polym. Ed.* 4:75–88, 1992.

[19] Park, K., F. W. Mao, and H. Park. Morphological characterization of surface-induced platelet activation. *Biomaterials* 11:24–31, 1990.

[20] Rechavia, E., M. C. Fishbein, and T. DeFrance. Temporary arterial stenting: Comparison to permanent stenting and conventional balloon injury in a rabbit carotid artery model. *Cathet. Cardiovasc. Diagn.* 41:85–92, 1997.

[21] Revak, S. D., C. G. Cochrane, B. N. Bouma, and J. H. Griffin. Surface and fluid phase activities of two forms of activated Hageman factor produced during contact activation of plasma. *J. Exp. Med.* 147:719–729, 1978.

[22] Richter, G. M., J. C. Palmaz, G. Noeldge, and F. Tio. Relationship between blood flow, thrombus, and neointima in stents. *J. Vasc. Interv Radiol.* 10:598–604, 1999.

[23] Rieu, R., P. Barragan, C. Masson, J. Fuseri, V. Garitey, M. Silvestri, P. Roquebert, and J. Sainsous. Radial force of coronary stents: A comparative analysis. *Catheterization Cardiovasc Interv.* 46:380–391, 1999.

[24] Talja, M., T. Valimaa, T. Tammela, A. Petas, and P. Tormala. Bioabsorbable and biodegradable stents in urology. *J. Urol. (Baltimore)* 11:391–397, 1997.

[25] Tamai, H., K. Igaki, E. Kyo, K. Kosuga, A. Kawashima, S. Matsui, H. Komori, T. Tsuji, S. Motohara, and H. Uehata. Initial and 6-month results of biodegradable poly-l-lactic acid coronary stents in humans. *Circulation* 102:399–404, 2000.

[26] Thakur, M. L., L. Walsh, H. L. Malech, and A. Gottschalk. Indium-111-labeled human platelets: Improved method, efficacy, and evaluation. *J. Nucl. Med.* 22:381–385, 1981.

[27] van Beusekom, H. M., D. M. Whelan, S. H. Hofma, S. C. Krabbendam, V. W. van Hinsbergh, P. D. Verdouw, and W. J. van der Giessen. Long-term endothelial dysfunction is more pronounced after stenting than after balloon angioplasty in porcine coronary arteries. *J. Am. Coll. Cardiol.* 32:1109–1117, 1998.

[28] Yamawaki, T., H. Shimokawa, T. Kozai, K. Miyata, T. Higo, E. Tanaka, K. Egashira, T. Shiraishi, H. Tamai, K. Igaki, and A. Takeshita. Intramural delivery of a specific tyrosine kinase inhibitor with biodegradable stent suppresses the restenotic changes of the coronary artery in pigs *in vivo*. *J. Am. Coll. Cardiol.* 32:780–786, 1998.

[29] Ye, Y. W., C. Landau, J. E. Willard, G. Rajasubramanian, A. Moskowitz, S. Aziz, R. S. Meidell, and R. C. Eberhart. Bioresorbable microporous stents deliver recombinant adenovirus gene transfer vectors to the arterial wall. *Ann. Biomed. Eng.* 26:398–408, 1998.

[30] Yuliang, J., H. Wu, R. B. Timmons, J. S. Jen, and F. E. Molock. Nonfouling surface produced by gas phase pulsed plasma polymerization of ultra-low-molecular-weight ethylene oxide containing monomer. *Colloids Surf., B* 18:235–248, 2000.